Physics Letters A 374 (2010) 3951–3956

Contents lists available at ScienceDirect

Physics Letters A

www.elsevier.com/locate/pla

A new car-following model with the consideration of the driver's forecast effect

T.Q. Tang [a,b,*], C.Y. Li [a], H.J. Huang [b]

[a] School of Transportation Science and Engineering, Beijing University of Aeronautics and Astronautics, Beijing 100191, China
[b] School of Economics and Management, Beijing University of Aeronautics and Astronautics, Beijing 100191, China

ARTICLE INFO

Article history:
Received 3 June 2010
Accepted 29 July 2010
Available online 4 August 2010
Communicated by A.R. Bishop

Keywords:
Car-following model
Driver's forecast effect
Traffic flow
Stability

ABSTRACT

In this Letter, we develop a new car-following model with the consideration of the driver's forecast effect (DFE). The analytical and numerical results show that the stability of traffic flow will gradually be enhanced with the increase of the forecast effect coefficient and the forecast time.

1. Introduction

Many traffic flow models have been developed to study various complex traffic phenomena (e.g. phase transition, lane-changing, etc.) [1–17]. However, these models cannot describe various complex phenomena resulted by the driver's forecast effect (DFE) since they did not consider this factor. The intelligent transportation system (ITS) can forecast the future traffic situation based on the current traffic status, so ITS will produce guidance information to driver. In order to study the effects of the guidance information on traffic flow, Tang et al. [18] proposed a macro model for traffic flow with the consideration of the DFE and found that the DFE can improve the stability of traffic flow, but they did not further study the micro influences of the DFE on the motion property of each vehicle. In this Letter, we develop a new car-following model with the consideration of the DFE and use this model to study the effects of the DFE on the stability of the car-following model.

2. Car-following model

The car-following model on one single lane can be reduced as follows [1]:

$$\frac{dv_n}{dt} = f(v_n, \Delta x_n, \Delta v_n), \tag{1}$$

where x_n, v_n are respectively the position and speed of the nth car, $f(\cdot)$ the stimulus function which depends on the headway $\Delta x_n = x_{n+1} - x_n$, the relative speed $\Delta v_n = v_{n+1} - v_n$ and the speed v_n. Later, scholars presented some extended optimal velocity models [6,7], i.e.

$$\frac{dv_n}{dt} = f(v_n, \Delta x_n, \Delta x_{n+1}, \ldots, \Delta x_{n+m}, \Delta v_n). \tag{2}$$

Zhao and Gao [8] found that the car-following model [5] will produce collision under some given conditions, then they presented a new car-following model, i.e.

$$\frac{dv_n}{dt} = f\left(v_n, \Delta x_n, \Delta v_n, \frac{dv_{n+1}}{dt}\right). \tag{3}$$

In order to further improve the stability of traffic flow, Wang et al. [9] developed a multi-velocity difference model, i.e.

$$\frac{dv_n}{dt} = f(v_n, \Delta x_n, \Delta v_n, \Delta v_{n+1}, \ldots, \Delta v_{n+k}). \tag{4}$$

The above models can describe some complex traffic phenomena, but they cannot be used to study the DFE since they did not consider the factor. ITS is very common in the real traffic system and can provide some forecast information to driver, so driver will adjust his acceleration based on the forecast information. Thus we can obtain a new car-following model with the consideration of the DFE, i.e.

$$\frac{dx_n(t+\tau)}{dt} = \beta_1 V\big(\Delta x_n(t)\big) + \beta_2 V\big(\Delta x_n(t+\tau_1)\big), \tag{5}$$

where β_1, β_2 are respectively the weights of the optimal velocities $V(\Delta x_n(t))$, $V(\Delta x_n(t+\tau_1))$, τ_1 is the forecast time. Eq. (5) shows

* Corresponding author at: School of Transportation Science and Engineering, Beijing University of Aeronautics and Astronautics, Beijing 100191, China. Tel.: +86 1082339327; fax: +86 82316009.
E-mail address: tieqiaotang@buaa.edu.cn (T.Q. Tang).

0375-9601/$ – see front matter
doi:10.1016/j.physleta.2010.07.062

that the nth car's acceleration at t is determined by the optimal velocity $V(\Delta x_n(t))$ and the optimal velocity $V(\Delta x_n(t+\tau_1))$, so it can be adopted to study some complex phenomena resulted by the traffic system with ITS.

In order to simplify Eq. (5), we carry out the Taylor expansion of the variables $\Delta x_n(t+\tau_1)$ and neglect the nonlinear terms, i.e.

$$\begin{aligned}\Delta x_n(t+\tau_1) &= \Delta x_n(t) + \tau_1 \frac{\mathrm{d}\Delta x_n(t)}{\mathrm{d}t} \\ &= \Delta x_n(t) + \tau_1 \Delta v_n(t). \end{aligned} \tag{6}$$

Thus $V(\Delta x_n(t+\tau_1))$ can be rewritten as follows:

$$V\big(\Delta x_n(t+\tau_1)\big) = V\big(\Delta x_n(t)\big) + \tau_1 \Delta v_n(t) V'\big(\Delta x_n(t)\big). \tag{7}$$

Thus, Eq. (6) can be rewritten as follows:

$$\frac{\mathrm{d}x_n(t+\tau)}{\mathrm{d}t} = V\big(\Delta x_n(t)\big) + \beta_2 \tau_1 \Delta v_n(t) V'\big(\Delta x_n(t)\big), \tag{8}$$

where β_2 can be called the forecast effect coefficient at this time.

In this Letter, we use the following optimal velocity [3]:

$$V(\Delta x_n) = \frac{v_{\max}}{2}\big[\tanh(\Delta x_n - h_c) + \tanh(h_c)\big], \tag{9}$$

where $v_{\max}$ is the maximum velocity and h_c is the safe distance.

The asymmetric difference method is often used to discretize the car-following model, so we here apply this method too. Thus, Eq. (8) is discretized as

$$\begin{aligned}\Delta x_n(t+2\tau) = \Delta x_n(t+\tau) &+ \tau\big[V\big(\Delta x_{n+1}(t)\big) - V\big(\Delta x_n(t)\big)\big] \\ &+ \tau_1\beta_2\big[V'\big(\Delta x_{n+1}(t)\big) - V'\big(\Delta x_n(t)\big)\big] \\ &\times \big[\Delta x_{n+1}(t+\tau) - \Delta x_{n+1}(t)\big] \\ &+ \tau_1\beta_2 V'\big(\Delta x_n(t)\big)\big[\Delta x_{n+1}(t+\tau) \\ &- \Delta x_{n+1}(t) - \Delta x_n(t+\tau) + \Delta x_n(t)\big]. \end{aligned} \tag{10}$$

3. Linear stability analysis

In this section, we study the linear stability of Eq. (8). The solution of the uniformly steady state of Eq. (8) can be written as follows:

$$x_{n,0}(t) = hn + V(h)t, \quad h = L/N, \tag{11}$$

where N is the number of cars, L is the length of the road and h is the average headway.

Let $y_n(t)$ be a small deviation from the uniform solution $x_{n,0}(t)$, $x_n(t) = x_{n,0}(t) + y_n(t)$, then, a linear equation can be obtained from Eq. (10),

$$\begin{aligned}\Delta y_n(t+2\tau) = \Delta y_n(t+\tau) &+ \tau V'(h)\big[\Delta y_{n+1}(t) - \Delta y_n(t)\big] \\ &+ \tau_1\beta_2 V'(h)\big[\Delta y_{n+1}(t+\tau) - \Delta y_{n+1}(t) \\ &- \Delta y_n(t+\tau) + \Delta y_n(t)\big], \end{aligned} \tag{12}$$

where $V'(h) = \frac{\mathrm{d}V(\Delta x)}{\mathrm{d}\Delta x}|_{\Delta x = h}$.

Let $\Delta y_n(t) = A\exp(ikn + zt)$, Eq. (12) can be rewritten as follows:

$$\begin{aligned}&e^{2z\tau} - e^{z\tau} - \tau V'(h)\big[e^{ik} - 1\big] \\ &- \tau_1\beta_2 V'(h)\big[e^{ik+z\tau} - e^{ik} - e^{z\tau} + 1\big] = 0. \end{aligned} \tag{13}$$

Solving Eq. (13) with respect to z, we find that the leading term of z is the order of ik. Since $z \to 0$ when $ik \to \infty$, z can be expressed by a long wave as $z = z_1(ik) + z_2(ik)^2 + \cdots$. Substituting it into Eq. (13) and neglecting the terms with order greater than 2, the two roots of z are obtained

$$z_1 = V'(h), \qquad z_2 = \frac{V'(h)}{2}\big[1 - 3V'(h)\tau + 2\beta_2\tau_1 V'(h)\big]. \tag{14}$$

Clearly, the flow becomes unstable if $z_2 < 0$ and stable if $z_2 > 0$. Thus, the demarcation curve between stable and unstable conditions (hereafter called the "neutral stability curve") is

$$\alpha = \frac{1}{\tau} = \frac{3V'(h)}{1 + 2\beta_2\tau_1 V'(h)}. \tag{15}$$

Thus, an unstable flow will evolve from a small perturbation in the uniform flow if the following condition holds

$$\alpha < \frac{3V'(h)}{1 + 2\beta_2\tau_1 V'(h)}. \tag{16}$$

Eq. (15) shows that the neutral stability curve will decrease with the forecast effect coefficient β_2 and the forecast time τ_1, so the stability of traffic flow will be improved with the increase of the forecast effect coefficient β_2 and the forecast time τ_1.

Fig. 1 shows the neutral stability curves in the space $(\Delta x, \alpha)$ under the different parameters (τ_1, β_2), where $\alpha = \frac{1}{\tau}$ is the sensitivity parameter. $V'(h)$ reaches the maximal value $\frac{v_{\max}}{2}$ at $h = h_c$, so the neutral stability curve has a critical point (h_c, α_c). Fig. 1 shows that α_c will decrease with the forecast effect coefficient β_2 and the forecast time τ_1, i.e. the DFE will pull down the neutral stability curve, so the stability region in the space $(\Delta x, \alpha)$ will be enlarged.

4. Nonlinear analysis

In order to further describe the effect of the parameters τ_1, β_2 on the stability of traffic flow, the nonlinear analysis is carried out to study the slowly varying behavior for the long waves in the stable and unstable regions. As for the space variable n and time variable t, we define the slow variables X and T as follows:

$$X = \varepsilon(n + bt) \quad \text{and} \quad T = \varepsilon^3 t, \tag{17}$$

where b is a constant determined. The headway is

$$\Delta x_n(t) = h_c + \varepsilon R(X, T). \tag{18}$$

Substituting Eqs. (17) and (18) into Eq. (10) and expanding Eq. (10) to the fifth order of ε, we can obtain the following nonlinear partial differential equation

$$\begin{aligned}&\varepsilon^2\big[b - V'\big]\partial_X R + \varepsilon^3 A_3 \partial_X^2 R + \varepsilon^4\big[\partial_T R + A_{41}\partial_X^3 R - A_{42}\partial_X R^3\big] \\ &+ \varepsilon^5\big[3b\partial_T\partial_X R + A_{51}\partial_X^4 R - A_{52}\partial_X^2 R^3\big] = 0, \end{aligned} \tag{19}$$

where

$$\begin{aligned}&V' = V'(h_c), \qquad V''' = V'''(h_c), \\ &A_3 = \frac{3b^2\tau}{2} - \frac{V'}{2} - \tau_1\beta_2 b V', \qquad A_{42} = A_{52} = \frac{V'''}{6}, \\ &A_{41} = \frac{7b^3\tau^2 - V' - \tau_1\beta_2 V'(3b + 3b^2\tau)}{6}, \\ &A_{51} = \frac{5b^4\tau^3}{8} - \frac{V'}{24} - \tau_1\beta_2 V'\left(\frac{4b + 6b^2\tau + 4b^3\tau^2}{24}\right). \end{aligned}$$

Setting $b = V'$, we can eliminate the second order term of ε from Eq. (19). We consider the neighborhood of the critical point τ_c, such that

$$\frac{\tau}{\tau_c} = 1 + \varepsilon^2, \tag{20}$$

where $\tau_c = \frac{1 + 2\beta_2\tau_1 V'(h_c)}{3V'(h_c)}$. Then Eq. (19) can be rewritten as follows:

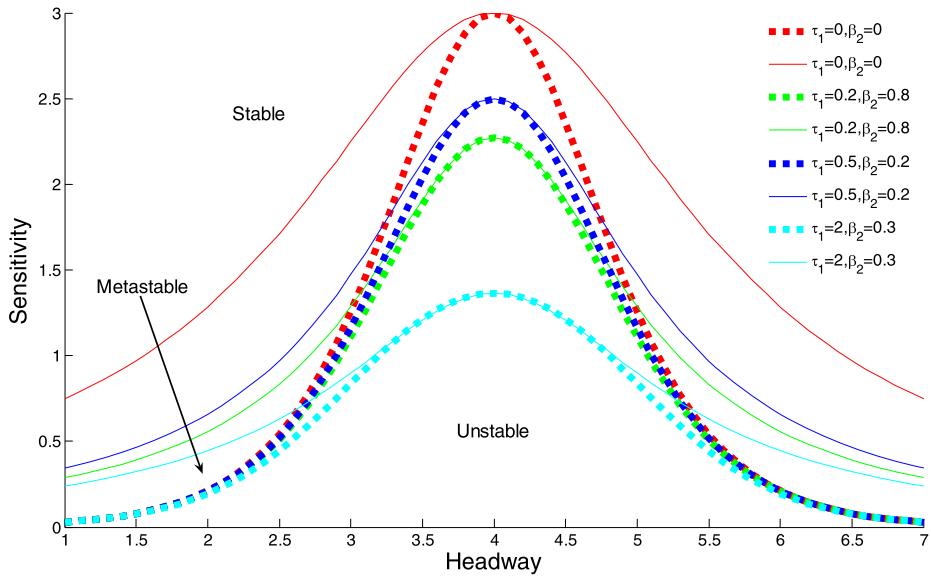

Fig. 1. Phase diagram in the head-sensitivity space $(\Delta x, \alpha)$. Each pair of parameters (τ_1, β_2) has a pair curves with the same maximum sensitivity, where the solid one is called the coexisting curve and the dash one is called the neutral stability curve. For each pair of curves, the space is divided into three regions: the stable region above the coexisting curve, the metastable region between the neutral and coexisting curves, and the unstable region below the neutral curve.

$$\varepsilon^4\left(\partial_T R - m_1\partial_X^3 R + m_2\partial_X R^3\right) + \varepsilon^5\left(m_3\partial_X^2 R + m_4\partial_X^2 R^3 - m_5\partial_X^4 R\right) = 0, \tag{21}$$

where

$$m_1 = -\frac{V'}{6}\left\{\frac{7}{9}\left(1+2\tau_1\beta_2 V'\right)^2 - 1 - \tau_1\beta_2 V'\left(4+2\tau_1\beta_2 V'\right)\right\},$$

$$m_2 = -\frac{V'''}{6}, \qquad m_3 = \frac{1+2\tau_1\beta_2 V'}{2}V', \qquad m_4 = \frac{V'''}{12},$$

$$m_5 = -\frac{5(1+2\tau_1\beta_2 V')^3}{216}V' + \frac{V'}{24} + \tau_1\beta_2 V'\left(\frac{36+18(1+2\tau_1\beta_2 V')+4(1+2\tau_1\beta_2 V')^2}{72}\right).$$

To derive the regularized equation, we make a transformation for Eq. (21), as follows:

$$\hat{T} = m_1 T, \qquad R = \sqrt{\frac{m_1}{m_2}}\hat{R}. \tag{22}$$

Then, Eq. (21) can be rewritten as the following regularized equation:

$$\partial_{\hat{T}}\hat{R} = \partial_X^3\hat{R} - \partial_X\hat{R}^3 - \varepsilon\sqrt{\frac{1}{m_1}}\left(m_3\partial_X^2\hat{R} + \frac{m_1 m_4}{m_2}\partial_X^4\hat{R} - m_5\partial_X^2\hat{R}^3\right). \tag{23}$$

Eq. (23) is the modified KdV equation after ignoring the perturbed term $O(\varepsilon)$. The kink solution of this equation is

$$\hat{R}_0(X,\hat{T}) = \sqrt{c}\tanh\left(\sqrt{\frac{c}{2}}(X - c\hat{T})\right), \tag{24}$$

where c is the propagation speed of the kink wave. This speed is determined by the $O(\varepsilon)$ term, which is solvable if

$$\left(\hat{R}_0, M[\hat{R}_0]\right) \equiv \int_{-\infty}^{+\infty} dX\,\hat{R}_0(X,\hat{T})M\left[\hat{R}_0(X,\hat{T})\right] = 0, \tag{25}$$

where

$$M[\hat{R}_0] = \sqrt{\frac{1}{m_1}}\left(m_3\partial_X^2\hat{R} + \frac{m_1 m_4}{m_2}\partial_X^2\hat{R}^3 - m_5\partial_X^4\hat{R}\right).$$

After integration, we can obtain the propagation speed

$$c = \frac{27(1+2\tau_1\beta_2 V')}{1+26\tau_1\beta_2 V' - 19(\tau_1\beta_2 V')^2 - 20(\tau_1\beta_2 V')^3}. \tag{26}$$

Thus, we have derived the solution of the mKdV equation, i.e.

$$R(X,T) = \sqrt{\frac{m_1}{m_2}}\tanh\sqrt{\frac{c}{2}}(X - m_1 cT). \tag{27}$$

If the optimal velocity takes the form (9), then $V' = 1$ and $V''' = -2$. The amplitude of the kink solution is given by

$$A = \left(\frac{m_1 c}{m_2}\left(\frac{\alpha_c}{\alpha} - 1\right)\right)^{1/2} \quad \text{with } \alpha_c = \frac{3V'}{1+2\tau_1\beta_2 V'}. \tag{28}$$

The kink wave solution represents the coexisting phase, which consists of the free flow phase and the congested phase and their headways are respectively equal to $\Delta x = h_c + A$, $\Delta x = h_c - A$. The coexisting curves under the different parameters (β_2, τ_1) are shown in Fig. 1. For each pair of parameters (β_2, τ_1), there are a pair of curves with the same maximal sensitivity α_c, where the upper curve is the coexisting one and the lower one is the neutral stability one. Each pair of curves will divide the space into three regions: the stable region above the coexisting curve, the metastable region between the neutral and coexisting curves and the unstable region below the neutral curve. In addition, we find that each pair of curves will decrease with the forecast effect coefficient β_2 and the forecast time τ_1, which shows that the stability region is enlarged and that the metastable and unstable regions are reduced. This further illustrates that considering the DFE can enhance the stability of traffic flow.

In order to further describe the impacts of the parameters (β_2, τ_1) on the stability of traffic flow, we study the relationship between the critical point α_c and the forecast effect coefficient β_2 and the relationship between the critical point α_c and the forecast time τ_1 (see Fig. 2). From Fig. 2, we find that α_c will decrease with the forecast effect coefficient β_2 and the forecast time τ_1, which further shows that the DFE can improve the stability of traffic flow.

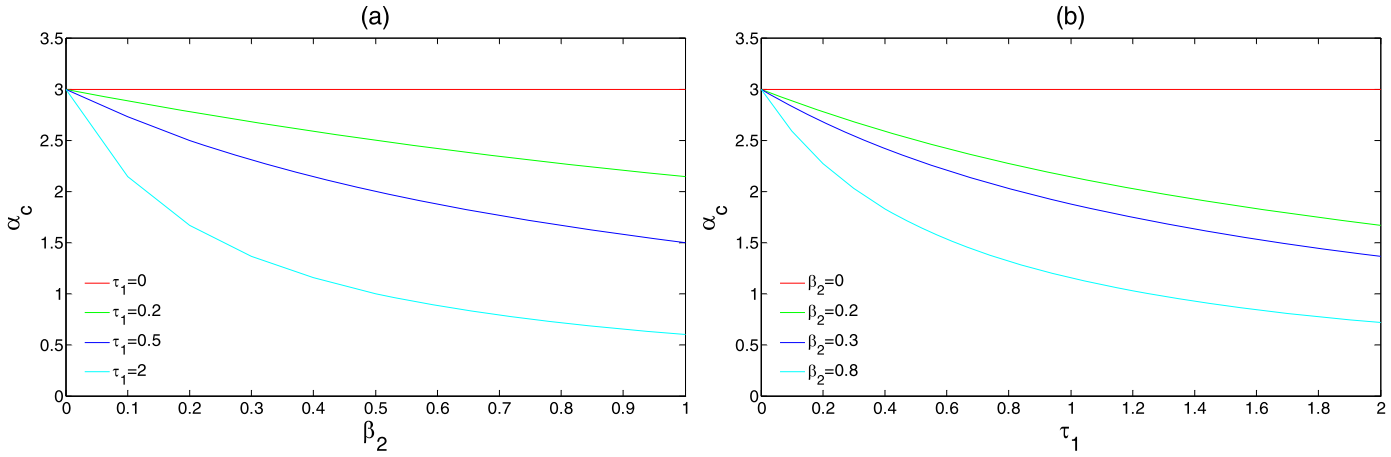

Fig. 2. The relationship between the critical point α_c and the forecast effect coefficient β_2 and the relationship between the critical point α_c and the forecast time τ_1.

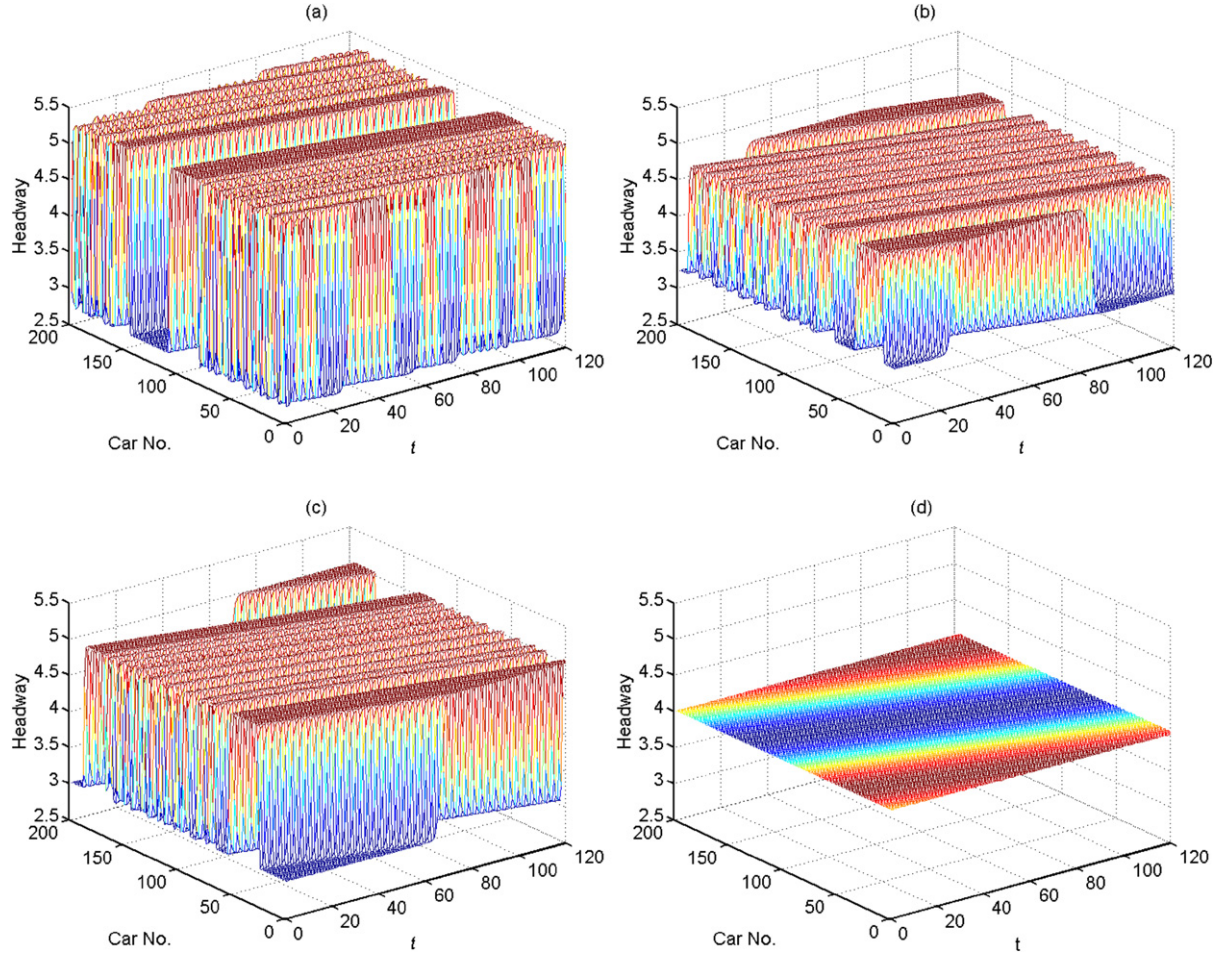

Fig. 3. The headway evolution after 10^4 time steps under the different parameters τ_1, β_2, where (a) $\tau_1 = 0$, $\beta_2 = 0$, (b) $\tau_1 = 0.2$, $\beta_2 = 0.8$, (c) $\tau_1 = 0.5$, $\beta_2 = 0.2$ and (d) $\tau_1 = 2.0$, $\beta_2 = 0.3$.

5. Simulations

In this section, we employ Eq. (8) to study the spatial–time evolution of the headway when small perturbation appears. The following initial conditions are adopted:

$$\begin{cases} \Delta x_n(0) = \Delta x_n(1) = \Delta x_0, & n \neq 0.5N,\ n \neq 0.5N+1, \\ \Delta x_n(0) = \Delta x_n(1) = \Delta x_0 + 0.1, & n = 0.5N, \\ \Delta x_n(0) = \Delta x_n(1) = \Delta x_0 - 0.1, & n = 0.5N+1, \end{cases} \tag{29}$$

where N is the number of vehicles and Δx_0 is the average headway. Periodic boundary condition is adopted in the simulation. Other parameters of the model are

$$v_{\max} = 2.0, \quad \tau = 0.5, \quad N = 200,$$
$$h_c = 4.0, \quad \Delta x_0 = 4.0. \tag{30}$$

Fig. 3 is the headway evolution after 10^4 time steps under the different parameters τ_1, β_2, where (a) $\tau_1 = 0$, $\beta_2 = 0$, (b) $\tau_1 = 0.2$,

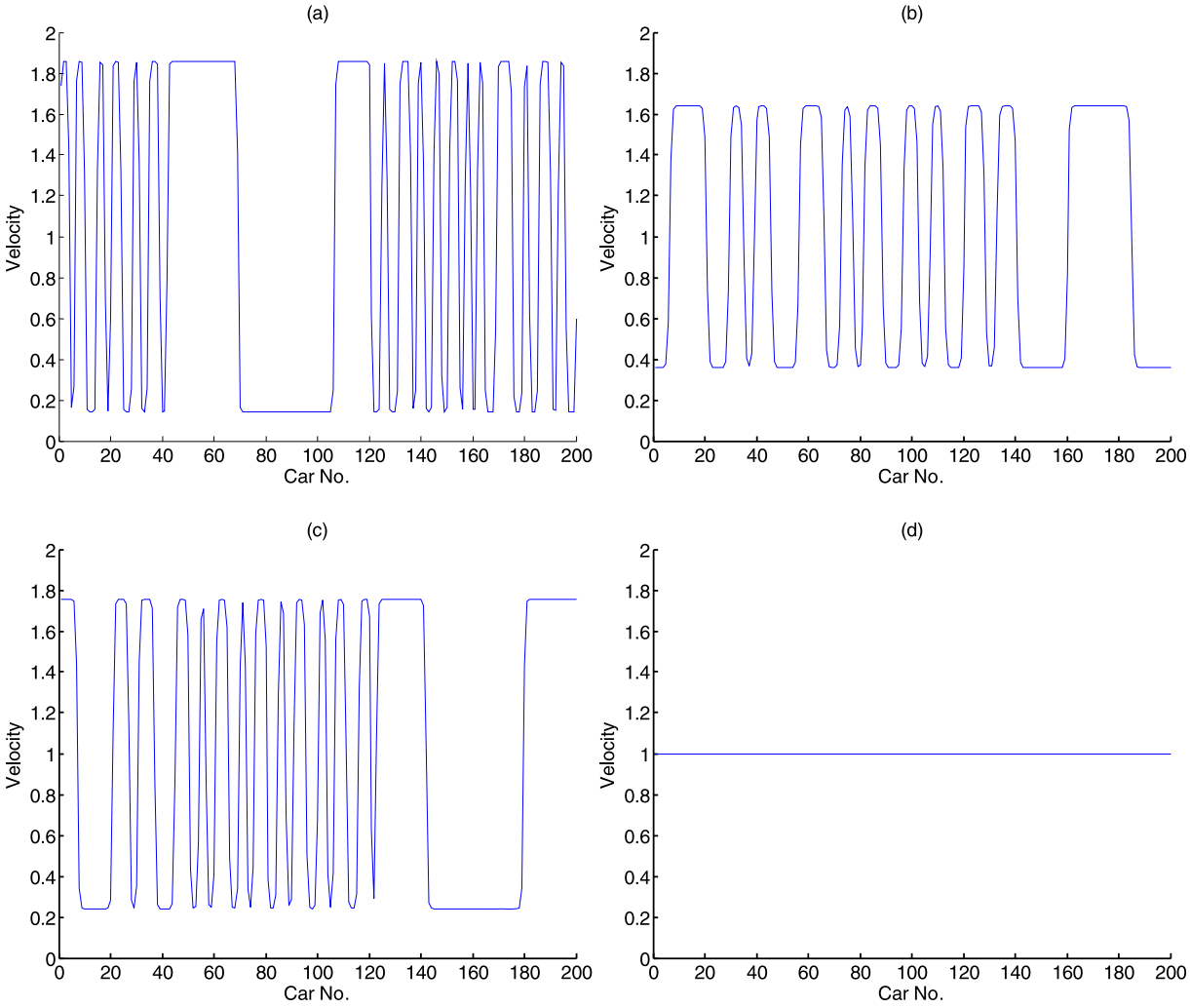

Fig. 4. The velocity profile at time step $t = 10^4$ under the different parameters τ_1, β_2, where (a) $\tau_1 = 0$, $\beta_2 = 0$, (b) $\tau_1 = 0.2$, $\beta_2 = 0.8$, (c) $\tau_1 = 0.5$, $\beta_2 = 0.2$ and (d) $\tau_1 = 2.0$, $\beta_2 = 0.3$.

$\beta_2 = 0.8$, (c) $\tau_1 = 0.5$, $\beta_2 = 0.2$ and (d) $\tau_1 = 2.0$, $\beta_2 = 0.3$. From Fig. 3, we can conclude the following results:

(i) In Figs. 3(a)–3(c), stop-and-go traffic appears. At this time, the headway evolution is very similar to the solution of the mKdV equation. This is because the initial value condition lies in the unstable region if we set τ_1, β_2 as $(0, 0)$, $(0.2, 0.8)$, $(0.5, 0.2)$. When a small perturbation is put into a uniform flow, the small perturbation will be amplified with time and the uniform flow will finally evolve into inhomogeneous flow. The stop-and-go in Fig. 3(a) is the most serious, followed by those in Figs. 3(b) and 3(c) since the DFE can improve the stability of traffic flow. In Fig. 3(d), the perturbation finally disappears.

(ii) Although Fig. 3 shows that the stability of traffic flow will be enhanced with the increase of the parameters τ_1, β_2, the stop-and-go resulted by the small perturbation (29) cannot completely be deleted if the forecast time τ_1 is relatively small (see Fig. 3(b)) or the forecast effect coefficient β_2 is relatively small (see Fig. 3(c)). This result shows that the stop-and-go resulted by the small perturbation (29) can completely be deleted only when drivers can enough consider the DFE (see Fig. 3(d)).

(iii) The density waves in Figs. 3(a)–3(d) always propagate backwards. This has been observed in reality and reported in relevant researches.

In order to further study the effects of the DFE on the stability of traffic flow, we describe the velocity profiles of the small perturbation (29) at $t = 10^4$ under the different parameters τ_1, β_2 (see Fig. 4). From Fig. 4, we can conclude the similar results to Fig. 3, which further illustrates that the DFE can improve the stability of traffic flow.

Figs. 3 and 4 show that the forecast time τ_1 and the forecast effect coefficient β_2 have great effects on the stability of traffic flow. In order to further describe these effects, we study the property of the phase space (τ_1, β_2) and find that the phase space (τ_1, β_2) can be divided into stable region and unstable region by a demarcation curve (see Fig. 5). From Fig. 5, we can conclude the following results:

(1) When the forecast time τ_1 is very small ($\tau_1 \leqslant 0.24$), the DFE cannot completely delete the stop-and-go resulted by the small perturbation (29) although the DFE can improve the stability of traffic flow (see Figs. 3(b), 4(b) and 5).
(2) Under the small perturbation (29), the demarcation curve is approximately the hyperbolic curve $\tau_1\beta_2 = 0.24$, so we find that the demarcation curve will decrease with the forecast effect coefficient β_2 and the forecast time τ_1, which shows that the stable region will increase with the forecast effect coefficient β_2 and the forecast time τ_1.
(3) When the parameters (τ_1, β_2) are above the demarcation curve, the DFE can completely delete the stop-and-go resulted by the small perturbation (29) (see Figs. 3(d) and 4(d)); the

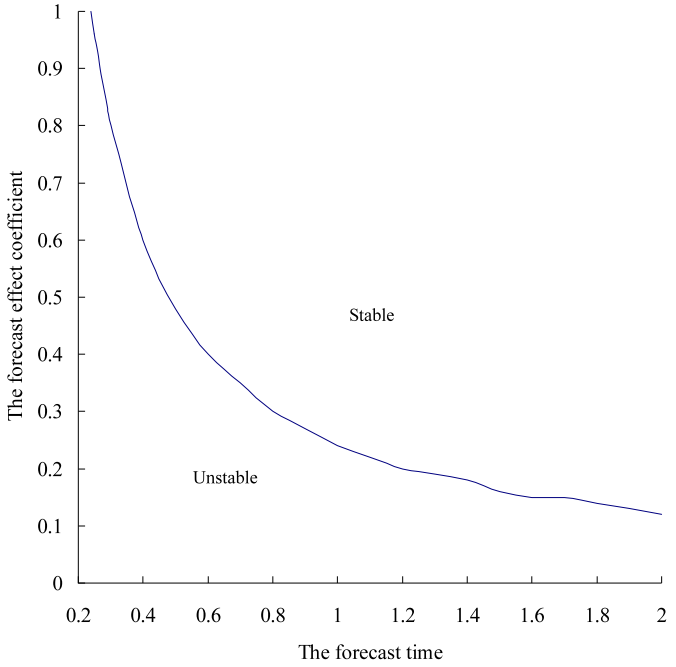

Fig. 5. Phase diagram in the space (τ_1, β_2).

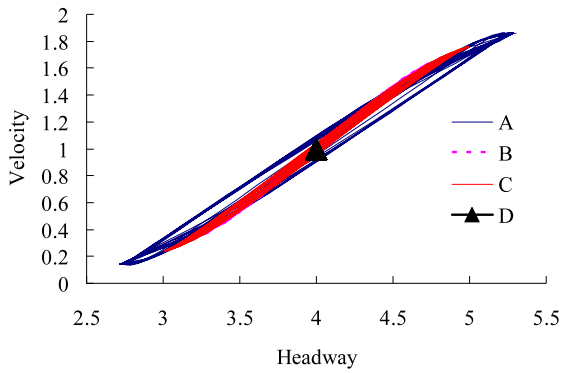

Fig. 6. The hystersis loops under the different parameters τ_1, β_2, where (A) $\tau_1 = 0$, $\beta_2 = 0$, (B) $\tau_1 = 0.2$, $\beta_2 = 0.8$, (C) $\tau_1 = 0.5$, $\beta_2 = 0.2$ and (D) $\tau_1 = 2.0$, $\beta_2 = 0.3$.

DFE cannot completely delete the stop-and-go resulted by the small perturbation (29) although the DFE can improve the stability of traffic flow when the parameters (τ_1, β_2) are under the demarcation curve (see Figs. 3(b), 3(c), 4(b) and 4(c)).

Finally, we use our model to analyze the effects of the DFE on the hysteresis loop (see Fig. 6). From Fig. 6, we find that the hysteresis loop will be reduced with the increase of τ_1, β_2 and that it will finally be reduced to a point, which further shows that the DFE can improve the stability of traffic flow stability and that the unstable traffic flow will completely be deleted only when drivers enough consider the DFE.

6. Conclusions

With the development of ITS, drivers can forecast the future traffic situation. However, the existing traffic flow models cannot be used to directly study the DFE since they did not consider this factor. In this Letter, we develop a new car-following model with the consideration of the DFE based on the properties of the car-following behavior. The analytical and numerical results show that the DFE can enhance the stability of traffic flow and that this stability will be improved with the increase of the parameters τ_1, β_2. In addition, the numerical tests show that the unstable traffic flow can completely be deleted only when drivers enough consider the DFE. However, the results obtained in this Letter are qualitative, so we should in the future combine many observed data to further investigate the inner relationship between the DFE and the stability of traffic flow.

Acknowledgements

This study has been supported by the Program for New Century Excellent Talents in University (NCET-08-0038), the National Natural Science Foundation of China (70701002, 70971007 and 70521001) and the National Basic Research Program of China (2006CB705503).

References

[1] D. Chowdhury, L. Santen, A. Schadschneider, Phys. Rep. 329 (2000) 199.
[2] D. Helbing, Rev. Modern Phys. 73 (2001) 1067.
[3] M. Bando, K. Hasebe, A. Nakayama, A. Shibata, Y. Sugiyama, Phys. Rev. E 51 (1995) 1035.
[4] D. Helbing, B. Tilch, Phys. Rev. E 58 (1998) 133.
[5] R. Jiang, Q.S. Wu, Z.J. Zhu, Phys. Rev. E 64 (2001) 017101.
[6] T. Nagatani, Phys. Rev. E 60 (1999) 6395.
[7] H.X. Ge, S.Q. Dai, L.Y. Dong, Y. Xue, Phys. Rev. E 70 (2004) 066134.
[8] X.M. Zhao, Z.Y. Gao, Eur. Phys. J. B 47 (2005) 145.
[9] T. Wang, Z.Y. Gao, X.M. Zhao, Acta Phys. Sinica 55 (2006) 634.
[10] M.J. Lighthill, G.B. Whitham, Proc. R. Soc. Lond. Ser. A 229 (1955) 317.
[11] P.I. Richards, Oper. Res. 4 (1956) 42.
[12] R. Jiang, Q.S. Wu, Z.J. Zhu, Transp. Res. B 36 (2002) 405.
[13] T.Q. Tang, S.C. Wong, H.J. Huang, P. Zhang, J. Adv. Transp. 43 (2009) 245.
[14] A.K. Gupta, V.K. Katiyar, Transportmetrica 3 (2007) 73.
[15] P. Bagnerini, M. Rascle, SIAM J. Math. Anal. 35 (2003) 949.
[16] G.C.K. Wong, S.C. Wong, Transp. Res. A 36 (2002) 827.
[17] D. Ngoduy, R. Liu, Physica A 385 (2007) 667.
[18] T.Q. Tang, H.J. Huang, H.Y. Shang, Phys. Lett. A 374 (2010) 1668.